Hot Working Of Heat Resistant Rapidly Solidified Al-Fe-V-Si Alloy

D. Shimansky and H.J. McQueen

Mech. Eng., Concordia University. Montreal, H3G 1M8, Canada

ABSTRACT

Isothermal hot torsion tests were performed on the rapidly solidified (RSP) aluminum alloys 8009 and FVS1212 (Al-12.4Fe-1.2V-2.3Si) over temperatures (T) of 300 to 600°C and at strain rates ($\dot{\varepsilon}$) from 0.1 to 4.0 s^{-1}. Due to deformation heating and possible partial dynamic recrystallization, prominent stress σ peaks occur in the equivalent $\sigma - \varepsilon$ curves. Increase of fracture strain with rise in T and with decrease of $\dot{\varepsilon}$ has been observed; however, ductility is very low in comparison with conventional aluminum alloys. The flow stress σ decreased gradually with declining $\dot{\varepsilon}$ ([sinh $\alpha\,\sigma$]^n function) and increasing T (Arrhenius). The activation energy for hot deformation was found to be much higher than those of pure aluminum and of some RSP alloys as a result of the high volume fraction of very fine $Al_{12}(Fe,V)_3Si$ dispersoids which are very resistant to coalescence. The alloy exhibits a linear correlation with α of slope s values in the Arrhenius plots and an inverse correlation between n and α. As a net result of the above two relationships, Q is independent of α. The optimum coefficient value was established for α =0.02MPa^{-1}. Comparisons are made to high temperature deformation of other RSP alloys.

Key words: rapid solidification, aluminum transition metal alloy, silicides, hot workability, constitutive analysis, creep resistance, dispersion strengthened

INTRODUCTION

Aluminum alloys 8009 (Al-8.5Fe-1.3V-1.7Si), otherwise designated FVSO812, and FVS1212 - (Al-12.4Fe-1.2V-2.3Si) are rapidly solidified, particle consolidated (RSP) alloys produced by Allied-Signal Co., USA. These alloys consist of very fine, nearly spherical $Al_{12}(Fe,V)_3Si$ (silicides) dispersoids formed from the decomposition of the rapidly solidified microstructures and uniformly distributed throughout the matrix. The superior elevated temperature strength/ stability of these alloys is due to the much slower coarsening rates of the silicides compared to the dispersoids found in the other high temperature RSP alloys. Also these alloys are almost devoid of coarse needle or platelike intermetallic phases which degrade alloy ductility and fracture toughness /1-4/. The high volume fractions of silicides and their desirable microstructural morphology make 8009 and FVS1212 very appealing for aerospace applications because of their high stiffness and light weight in combination with advantageous elevated temperature mechanical properties while retaining a fracture toughness/strength level comparable to that of the 2000 and 7000 series and Ti aerospace alloys /2,5-7/.

Understanding of high T deformation behavior of 8009 and FVS 1212 is critical in designing suitable hot working conditions used in powder consolidation and secondary fabrication of this RSP alloy, having notably high strength and limited ductility consistent with its creep resistance. Hot torsion is a suitable method because it has the advantage, in comparison to tension and compression, of covering a large range of strains as used in forging and extrusion /8-15/. Although high strains can be achieved at a constant strain rate, there is a linear variation of strain and strain rate from zero at the centre to maximum at the surface. Nevertheless, hot torsion testing of solid cylindrical specimens is reliable in determining optimum hot working parameters such as strain, strain rate $\dot{\varepsilon}$ and temperature T /5-15/. In addition, torsion can rapidly simulate potential thermomechanical processes in order to improve the toughness.

TORSION TESTING

Specimens machined out of rods, extruded from consolidated powder, were deformed on a servo-controlled, closed loop torsion machine /5-7, 11-14/. In this MTS computer-directed system, torque is applied to a specimen through a rotary hydraulic actuator mounted on a converted lathe bed. On the torsional frame, the test piece is held by coaxial superalloy bars with attached grips. One end of the specimen is twisted a measured amount by the hydraulic motor controlled by a servo-valve while the other end is held fixed by a torque cell /12-14/. Continuous isothermal tests at 300, 400, 500 and 600°C were conducted at strain rates of 0.1, 1.0 and 4.0 s^{-1}.

Specimens are heated by a quadruple elliptical radiant furnace connected to a programmable controller with varied power input. The water-cooled furnace is capable of 1200°C with rapid heating rates. A transparent quartz tube passing through the furnace encloses the specimen, grips and bars, being sealed to fixtures cooling the grips. Argon is circulating through the tube during heating and testing to prevent oxidation. The temperature is measured by an alumel-chromel (K-type) thermocouple, insulated with double bore ceramic tubing, extending along the stationary test piece shoulder and attached to the specimen with alumel-chromel wire to maintain thermal contact. The mechanical attachment of the thermocouple tip to the gauge section at the fixed end gave a satisfactory thermal contact, yet underwent only a small fraction of the revolutions without suffering damage /5,12-14/.

The materials used in the present study are commercially designated as 8009 (FVS 0812) and FVS 1212 with chemical compositions: Al-8.5Fe-1.3V-1.7Si and Al-12.4Fe-1.2V-2.3Si, respectively. Torsion specimens with axes parallel to the rolling or extrusion direction were machined to close tolerances, especially in the gauge section, in order that twisting would be uniform. One end of the test piece is threaded, while the other end has a rectangular section which fits into a slot. This arrangement allows for easy mounting and removal without accidentally straining the specimen. Before starting any test, the reflecting surfaces of the furnace were cleaned with gauze so that the test temperature would be reached as quickly as possible. Every specimen was heated to the desired temperature and held constant ten minutes prior to deformation. For both materials, the samples were twisted without interruption to either fracture ε_f or to a strain of approximately 2.5. Specimens were quenched in water less than ten seconds after deformation was completed /5/.

RESULTS

Torsion testing data are usually recorded in the form of torque (M) versus angle of twist (θ) diagrams. These curves are converted to stress (σ) -strain (ε) curves, equivalent, according to von Mises criteria, to those in uniaxial compression or tension, using the following equations [10-14].

$$\sigma = \sqrt{3}M(3+m+N)/(2\pi r^3) \quad (1)$$

$$\varepsilon = r\theta / \sqrt{3}L \quad (2)$$

where r and L are the gauge radius 2.54 and gauge length 20.3 of the specimens, respectively, and m and N are strain rate sensitivity and strain hardening rate. The former is determined from M versus $\dot{\varepsilon}$ diagrams (Fig. 1) and the latter is set to zero accurate at the peak but in error by at most 5% elsewhere. The equivalent stress σ -equivalent strain ε graphs produced from hot torsion are shown in Fig. 2. To summarize directly the dependence at each $\dot{\varepsilon}$, peak stress versus T and ductility as strain to fracture ε_f versus T are shown in Fig. 3 and Fig. 4. The peak stress σ data were fitted to the following constitutive equation [5-7,9,10-14]:

$$A(\sinh \alpha\sigma_p)^n = \dot{\varepsilon} \exp(Q/RT)=Z \quad (3)$$

where A, a, n and Q are materials constants. The value of α was varied from 0.02 to 0.08 MPa^{-1}, including 0.052 commonly used to analyze Al alloys to permit comparison of activation energies and graphical presentations. The optimum value of should bring close to parallel the constant T lines (slope n in Fig. 5 and Fig. 6) and the constant $\dot{\varepsilon}$ lines in the Arrhenius plots (slope s in Fig. 7 and Fig. 8) [5-7]. From these plots Q is calculated using the following relationship:

$$Q = 2.3 \bullet R \bullet n \bullet s \quad (4)$$

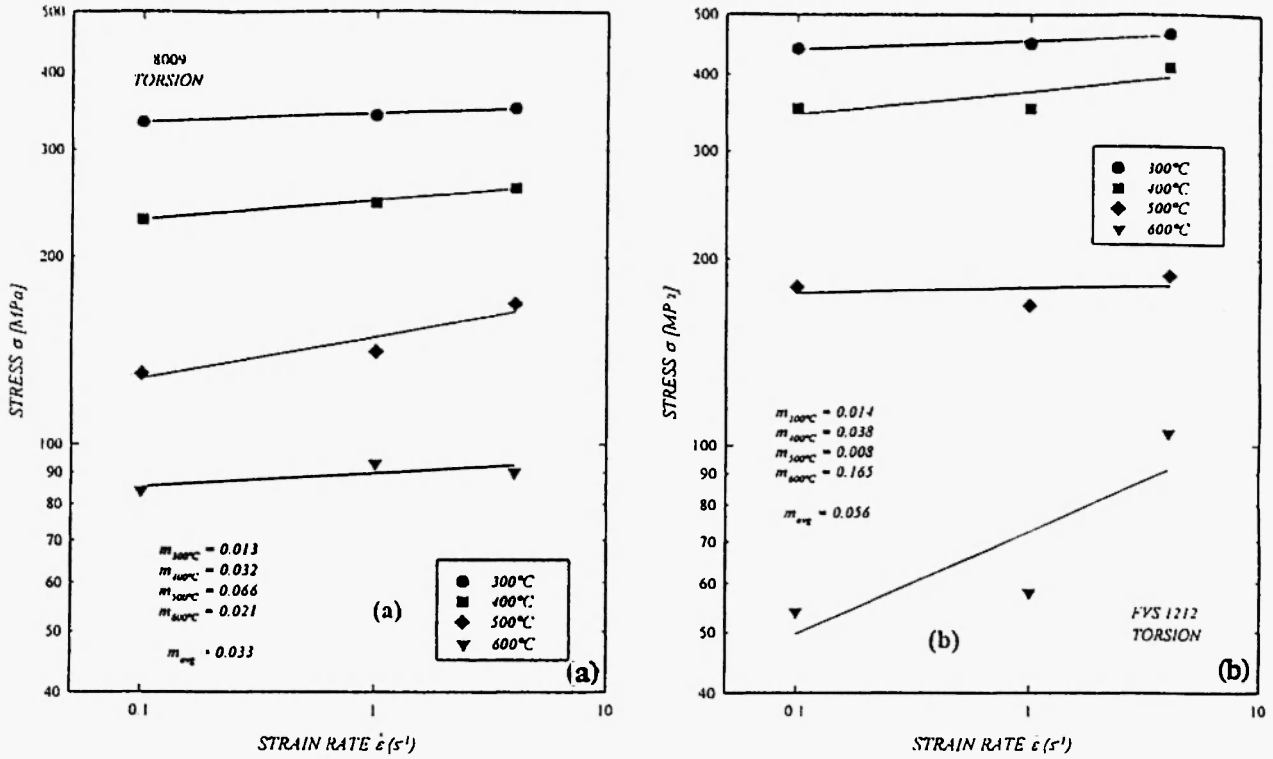

Fig. 1: Plot of log torque versus log (surface $\dot{\varepsilon}$) in order to determine the slopes m for use in Eq. 1 to calculate surface stress σ.

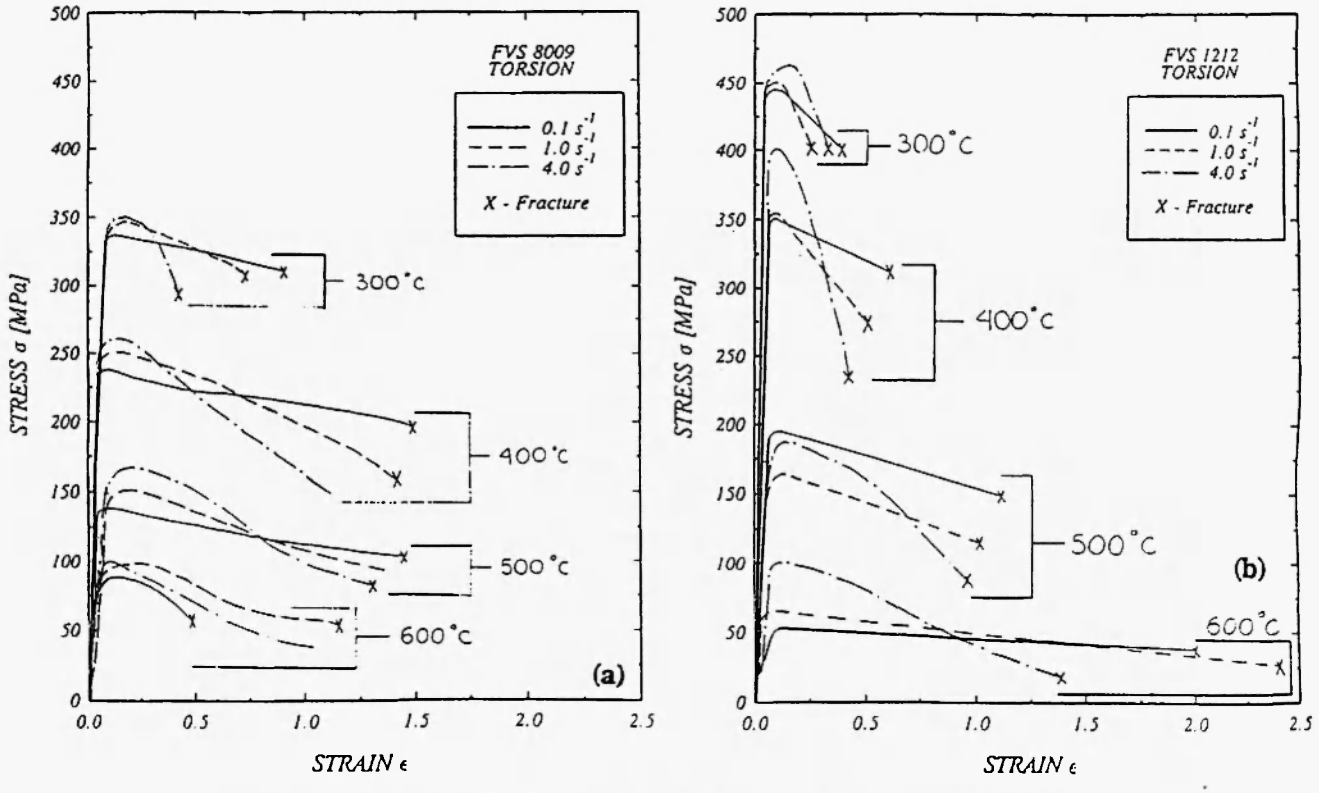

Fig. 2: Equivalent stress-strain curves for (a) 8009 and (b) FVS1212. /5-7/.

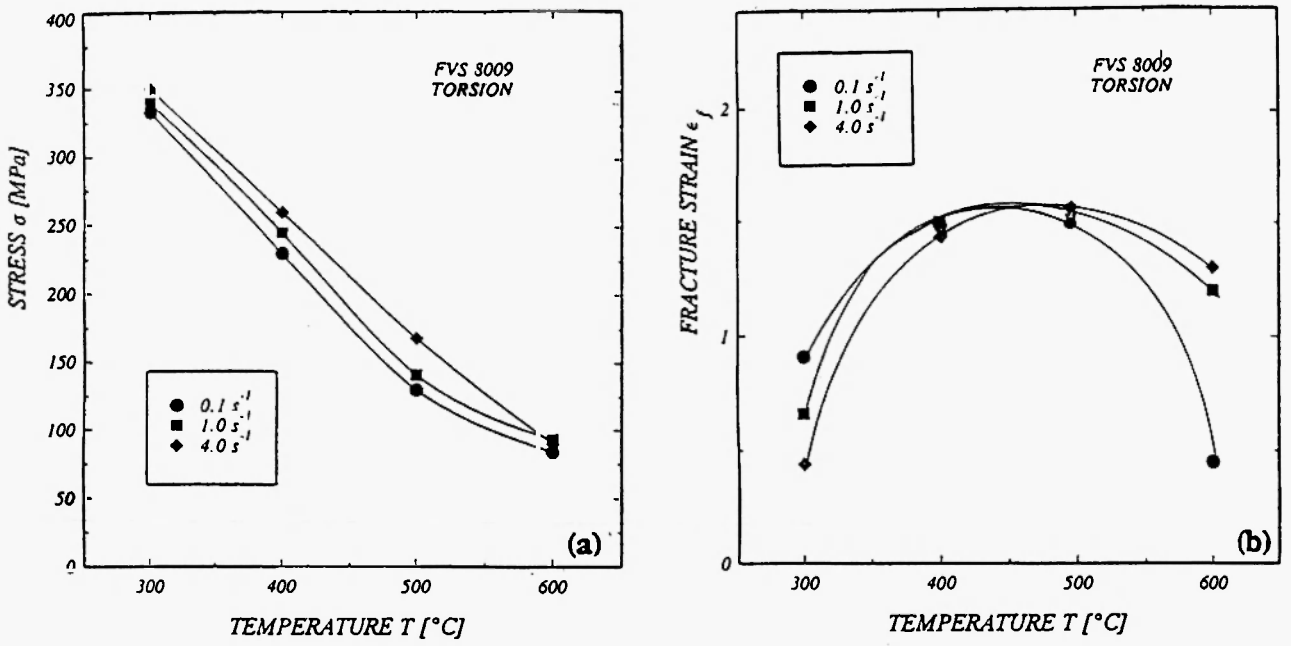

Fig. 3: Equivalent peak stress (a) and fracture strain (ductility) (b) versus temperature for 8009 alloy /5,6/.

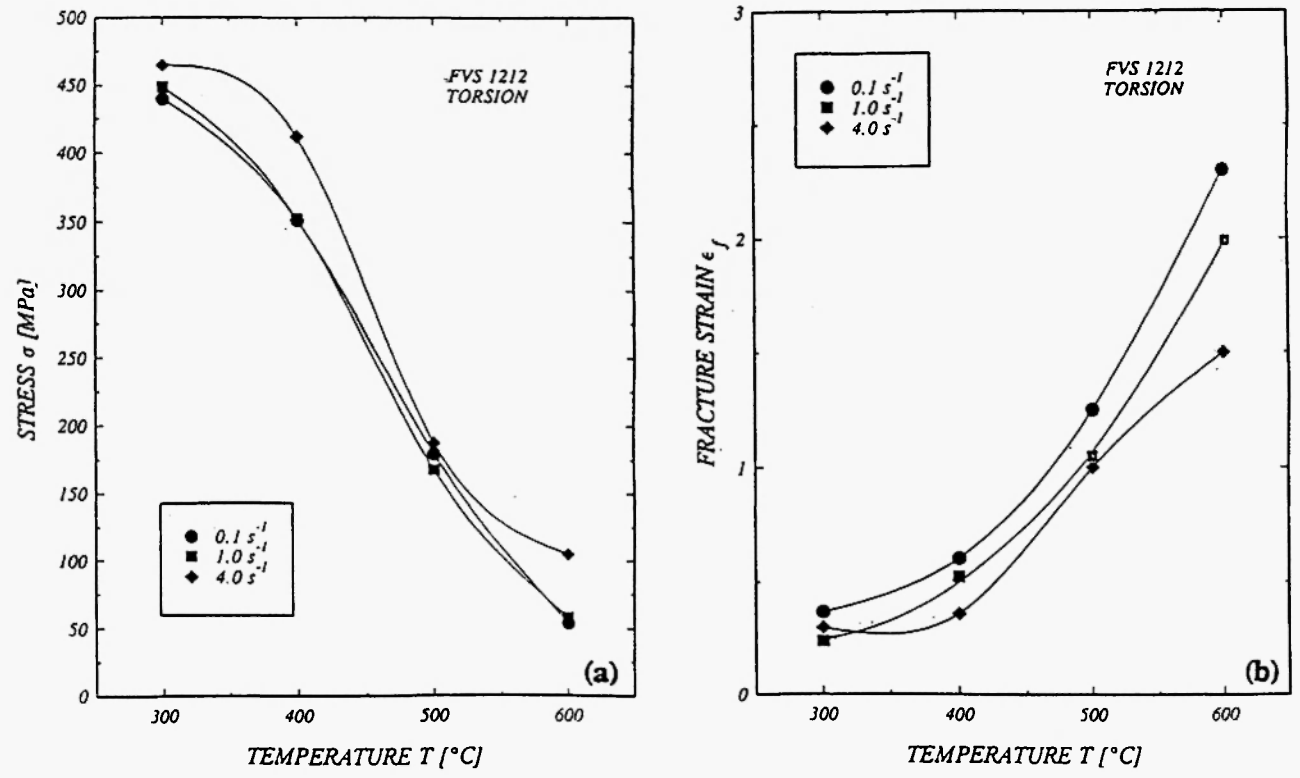

Fig. 4: Equivalent peak stress (a) and fracture strain (duc ility) (b) versus temperature for FVS1212 alloy /5,7/.

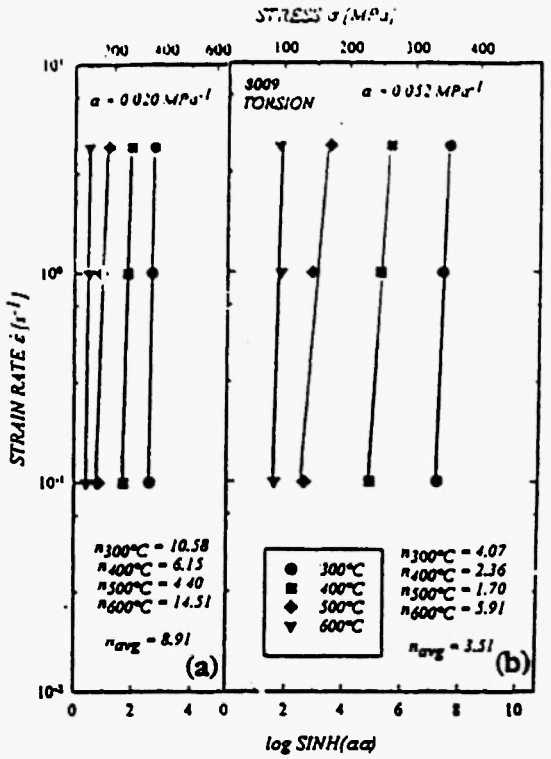

Fig. 5: Constitutive plots for 8009, log $\dot{\varepsilon}$ versus log sinh $\alpha\sigma$ with slope n a) for α = 0.02 MPa-1 and (b) for α= 0.052 MPa-1 /5,6/.

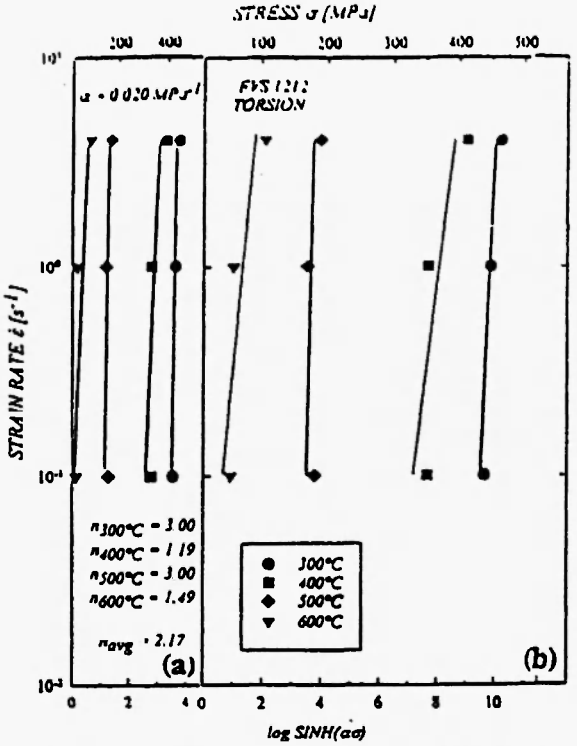

Fig. 6: Log strain rate versus log sinh ($\alpha\sigma$) for FVS1212 at (a) α = 0.02 MPa-1; and (b) α = 0.052 MPa-1 [5,7].

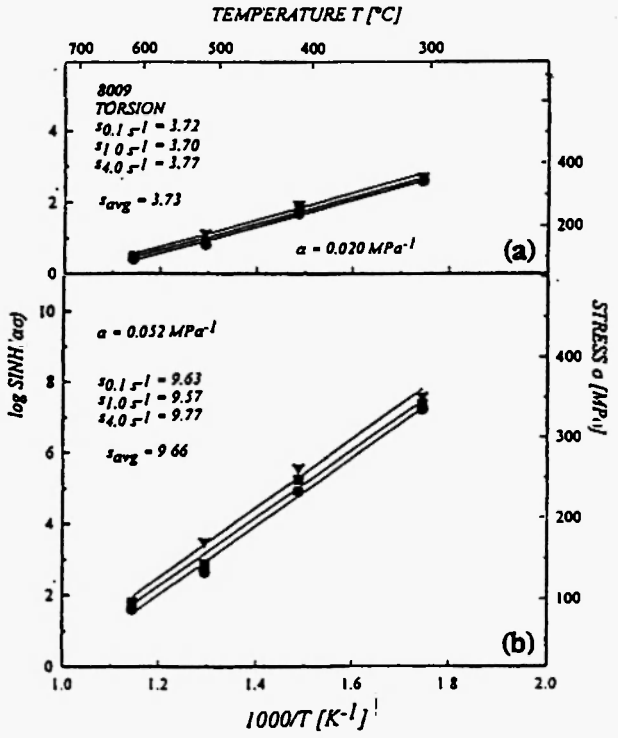

Fig. 7: Arrhenius plot for 8009 with slope s at (a) α=0.02 MPa-1; and (b) α = 0.052 MPa-1 /5,6/.

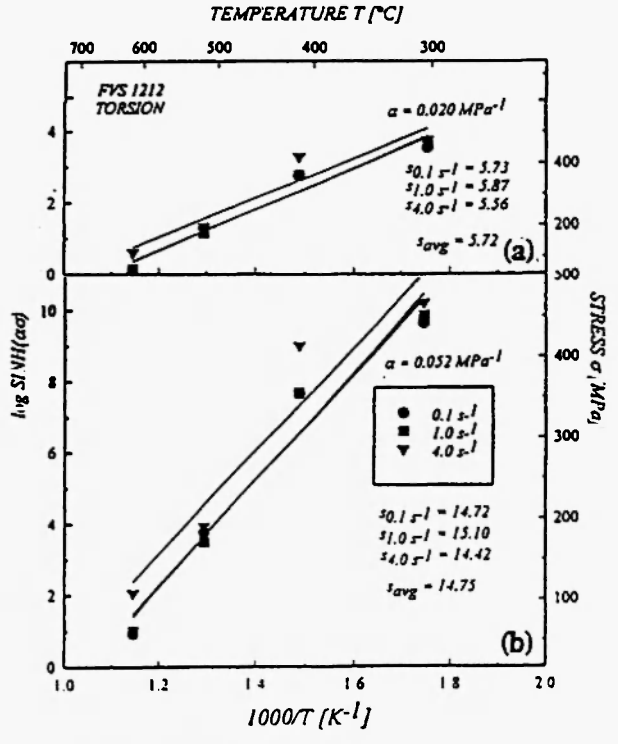

Fig. 8: Arrhenius plots for FVS1212 at (a) α = 0.02 MPa-1; and (b) α = 0.052; MPa-1 [5,7].

The variations of n, s and Q versus α are summarized in Fig. 9 and Fig. 10 for each alloy. The plots of s versus α show direct proportionality with constants 186 MPa and 286 MPa, while n is proportional to the reciprocal of α with the constants of 0.180 MPa^{-1} and 0.675 MPa^{-1} for 8009 and FVS1212, respectively. For 8009, the value of Q increases slightly with rising α from 636 to 650 kJ/mol. For FVS1212, the value of Q at α = 0.01 MPa^{-1} is at its low of 612 kJ/mol; it rises to 673 kJmol at α = 0.04 MPa^{-1} and falls to 633 kJ/mol at α 0 = 0.08 MPa^{-1}. The stress data obtained for all temperatures and strain rates can be correlated to the Zener-Hollomon parameter (Z), a temperature compensated strain rate (Fig. 11 and Fig. 12) /5-7/.

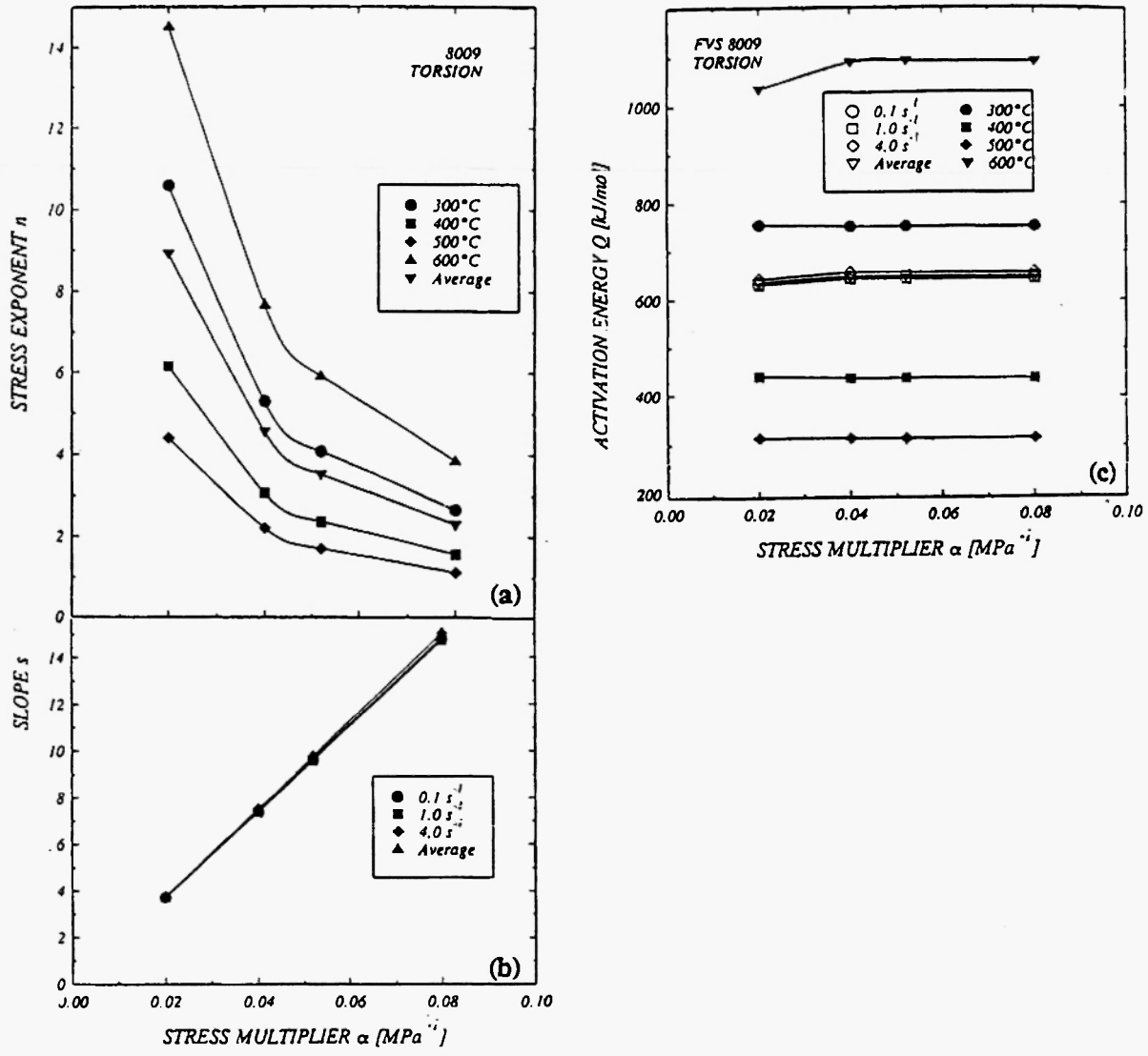

Fig. 9: Variation with stress multiplier α of (a) stress exponent n; (b) Arrhenius slope s and (c) activation energy Q for 8009 alloy /5,6/.

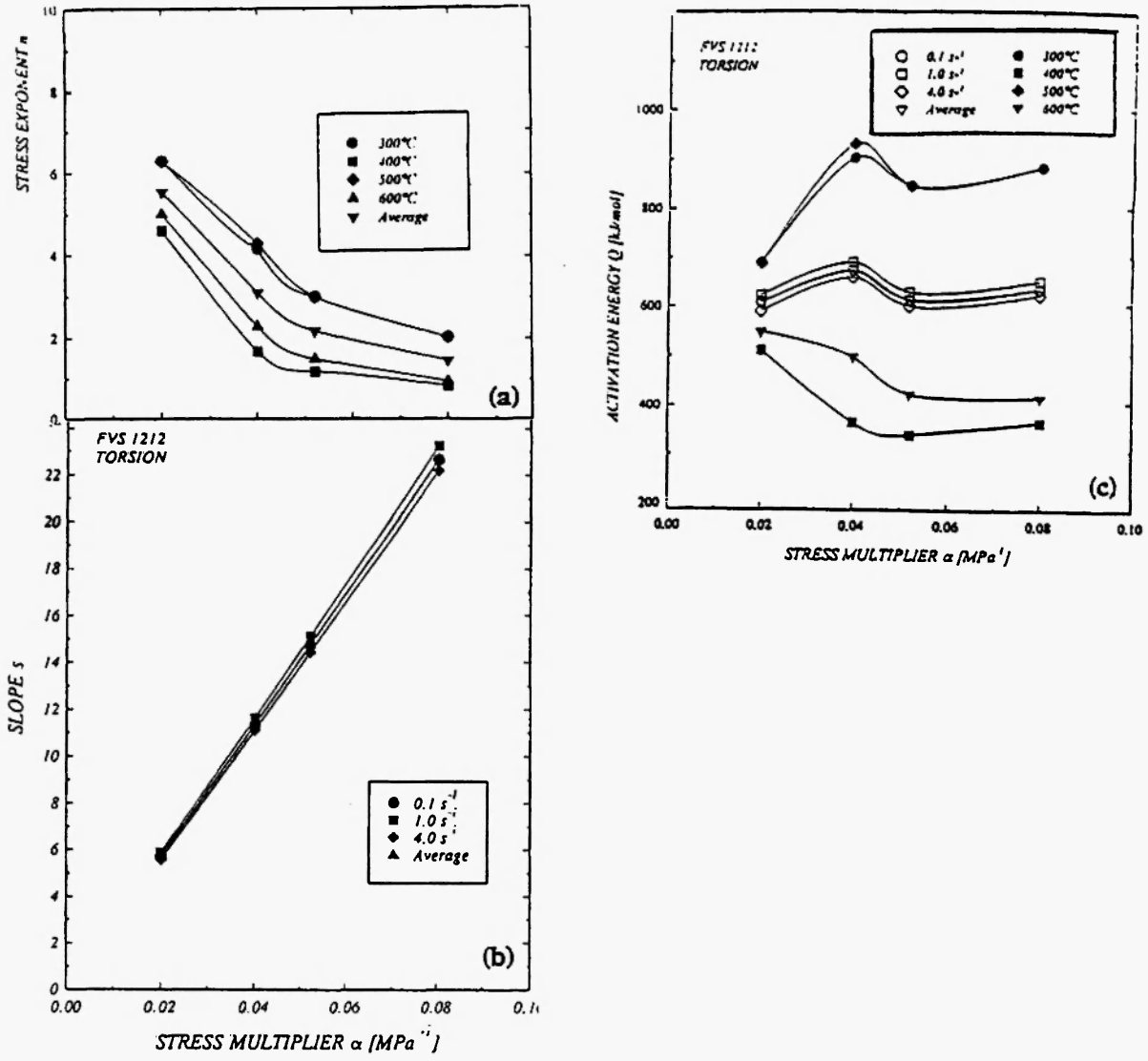

Fig. 10: For FVS1212: (a) stress exponent n; (b) Arrhenius slope s and (c) activation energy Q versus stress multiplier α/5,7/.

DISCUSSION

From the $\sigma - \varepsilon$ curves at each T for both alloy 8009 and FVS 1212 /5-7/ the degree of softening beyond the stress peak increases as $\dot{\varepsilon}$ rises, which indicates that deformation heating plays a significant role. With increase in T, the drop in stress with strain generally becomes more gradual although the total decline may be greater because of the higher ductility. For the leaner alloy, (8009, FVS0812) the flow curves at 300°C are lower but those at 500°C are higher than for FVS1212, thus lowering the slopes of the Arrhenius curves. The flow curves at 500 and 600°C in FVS 1212 and at 400 to 600°C in 8009 tend to turn towards the horizontal, indicating that there is a microstructural effect in the softening. Structural changes, such as precipitate transformation and coarsening /15-18/, have been shown to be insignificant /1-4/. Dynamic recrystallization (DRX) related to the particles may cause the softening /13,18/. However, the increase of peak strain with declining T is unusually low; this may be due to DRX becoming less influential while

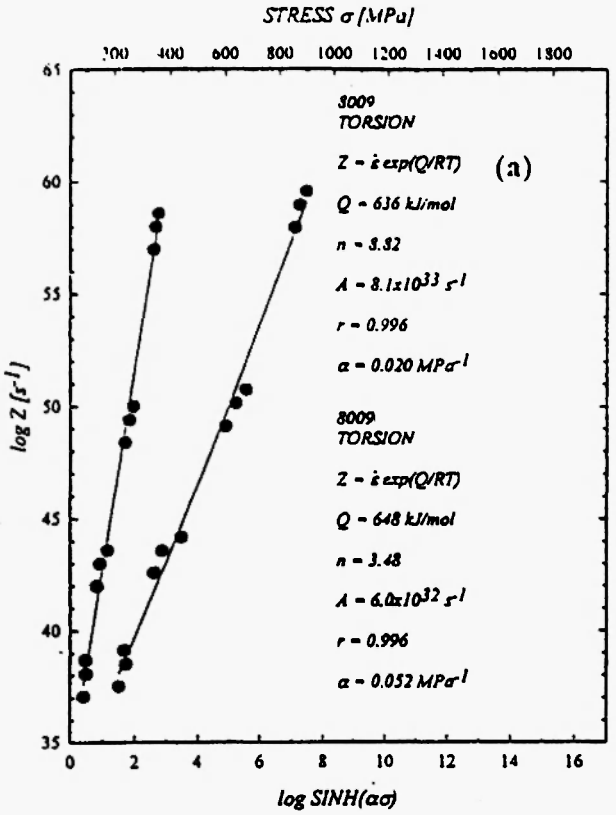

Fig. 11: Log Zener-Hollomon parameter versus log sinh ασ for 8009 at α= 0.02 and 0.06MPa^{-1} /5,6/.

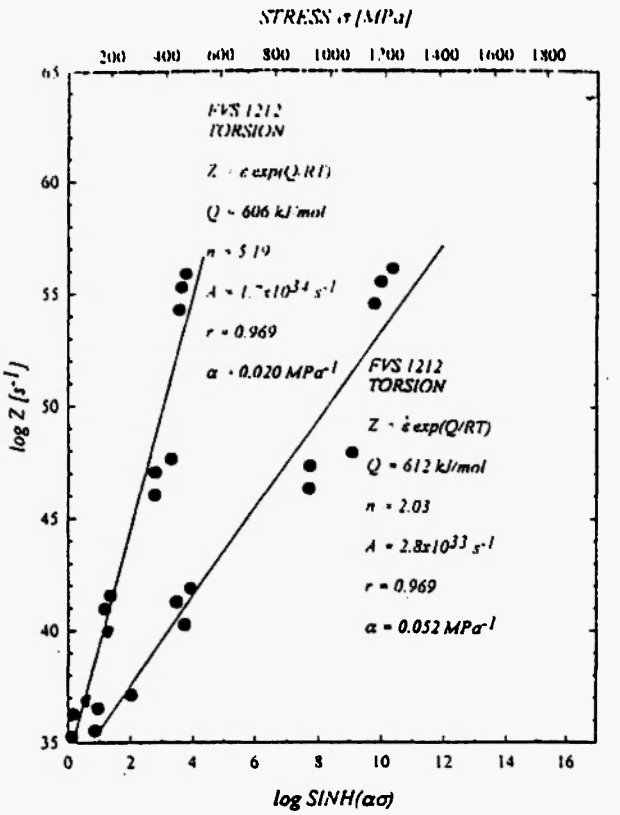

Fig. 12: Log Zener-Hollomon parameter versus log sinh (ασ) for FVS1212 at α = 0.02 MPa-1 and α = 0.06 MPa^{1} /5,7/.

deformation heating becomes increasingly important.

For the interdependence of σ and $\dot{\varepsilon}$, the hyperbolic sine equation gives a suitable fit to the data /5-7/. While the best fit is at α = .020 MPa^{-1} and n = 8.91 for 8009 or n = 5.54 for FVS 1212, the other values of α give only a slight decrease in quality as can be seen in Fig. 5 or Fig. 6. The s values for 8009 are much less than those of FVS 1212 (Fig. 7 and Fig. 8), indicating a lower dependence on T as one would expect; however, the values of n for 8009 are much higher with the net result that Q ranged from 636 to 650 kJ/mol as increased from 0.02 to 0.08 MPa^{-1} /5-7/. The Q values of 612 kJ/mol for FVS 1212 are much higher than that of self diffusion which governs the climb of edge dislocations in pure Al /10,18/. This may be due to the interactions between dislocations and the silicides which are extremely stable and are essentially insoluble /1-4/; they act as obstacles to the cross slip and climb of dislocations and pin the subboundaries. High activation energies of about 290kJ/mol arose in Al-0.65Fe and Al-0.5Fe-0.5Co from fine highly stable eutectic rods /14/. These serve as strong obstacles to dislocation bypassing at 200 and 300°C so that they strongly pin the subboundaries. Possibly part of the increase in the Q value may be due to the participation of dynamic recrystallization which initiates at higher σ and ε as T decreases /9,13,20/.

Figure 13 presents, for comparison over a range of temperatures, the yield strengths of several industrial RSP alloys, including FVS1212 and FVS0812(8009) as well as their hot torsion test results /2,5-7/. In the range 300 to 400°C, FVS 1212 almost matches the performance of titanium alloy Ti-6Al-4V. The creep results in the range 10^{-8} -10^{-4} s^{-1}, 314-379°C for FVS 1212 provided an activation energy of 360 kJ/mol /21/. The creep results for Al-8.8Fe-3.7Ce, when analyzed in the same way, also indicated Q = 360 kJ/mol /22/. The variations in mechanisms responsible for the

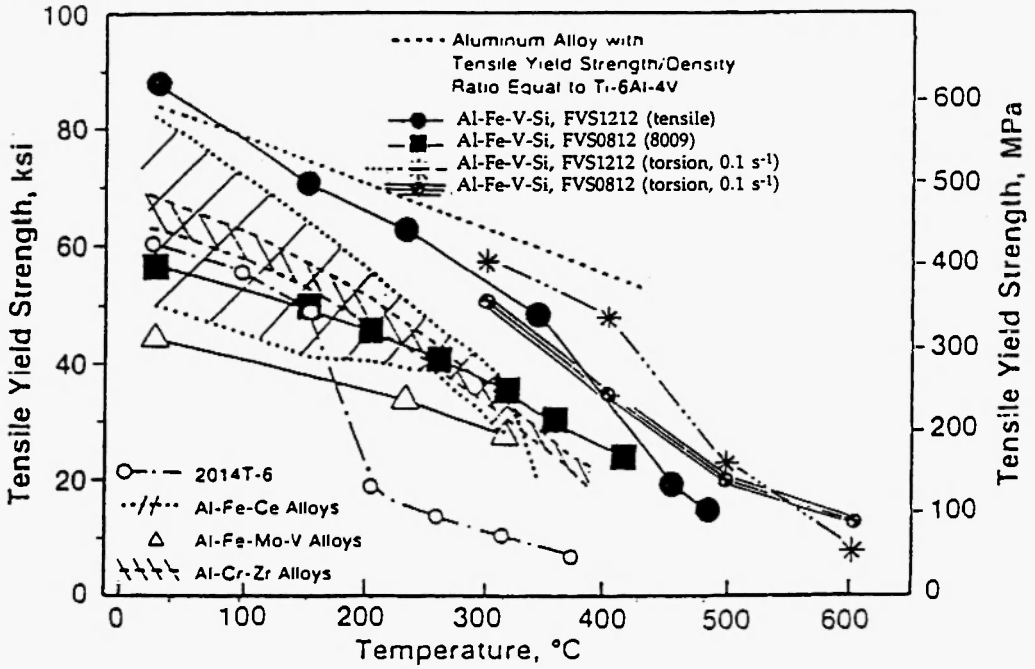

Fig. 13: Comparison of elevated temperature tensile yield strengths of various high temperature and standard aerospace alloys /2/. Torsion peak stress for two Al-Fe-V-Si alloys /5-7/.

differences in the activation energies from creep to hot working are not known because of insufficient microstructural investigation; however, larger Q values at higher stresses are not uncommon. A more extensive survey and discussion of the relative high T strength and stability of rapidly solidified, transition-element alloys has been published /23/.

In 8009 the ductility increased from 300 to 400°C but then declined from 500 to 600°C; the possibility of enhanced grain boundary cracking will be examined by microscopy. The ductility of FVS 1212 rose with rising T and decreasing $\dot{\varepsilon}$ in the common manner for hot working. While at or below 500°C it was less ductile than 8009 alloy, it was remarkably more ductile at 600°C where it is also softer. While this has not been confirmed by metallography, one could possibly attribute such behavior to superplastic effects in the FVS 1212 which likely has a very fine grain size due to the high particle content; the strain rate sensitivity reaches 0.165 for this condition five times higher than other conditions and for 8009 /5-7/.

In hot torsion tests of RSP alloy Al-20Si-7.5Ni-3Cu-1Mg, the flow curves exhibit a peak and softening to a steady state regime /24,25/. Microscopy confirmed that DRX occurred and showed that this alloy has 30% dispersoids with a variety of compositions and sizes compared to FVS1212 with 36% and to 8009 with only 24% uniform thermally-stable fine (30-80 mm diameter) spherical dispersoids that are less likely to stimulate nucleation. The ductility rises uniformly with rising T and declining $\dot{\varepsilon}$. It is greater than those of 8009 and FVS 1212 below 500°C; in the present alloys, the DRX is more restricted and less able to reduce stress concentration. In the Al-20Si-7.5Ni-3Cu-1Mg, the sinh constitutive equation showed the best fit for $\alpha = 0.015$ MPa^{-1} and $n = 2.46$ with a low Q of 233 kJ/mol /24,25/ that could result form the narrow range of 350 to 450°C compared to the present tests. At 400°C, 0.1 s^{-1}, the peak flow stress was only 100 MPa compared to 350 MPa for FVS 1212 and 235 MPa for 8009 /5,6/ . The flow curve of Al-Si-Ni-Cu at 450°, 0.083 s^{-1} is almost horizontal at 30 MPa in similarity to that of FVS 1212 having 50 MPa at 600°C, 0, 1 s^{-1}; in association with this, strain rate sensitivity at 425°C is 0.24 /24/.

Hot torsion results have been reported for RSP alloys Al-9Fe and Al-14Fe in the ranges 400 to 550°C and 7×10^{-3} to 5×10^{-2} s^{-1} /26/. The flow curves

exhibited peaks followed by work softening and the microstructure gave evidence of DRX. At the highest T and lowest $\dot{\varepsilon}$, the ductility reached 3 with almost constant flow stresses of 20 and 30 MPa for the 9 and 14% Fe respectively; the strain rate sensitivity had increased to 0.32 from a low of 0.20 at the lowest T. At 550°C, 0.05 s^{-1}, the flow stresses were between 35 and 45 MPa. The power law constitutive constants were n = 3.64 and 4.53 and Q = 161 and 180 kJ/mol for Al-9Fe and Al-14Fe respectively; the low values of Q are not consistent with other RSP alloys.

CONCLUSIONS

- The hot working behavior of 8009 and FVS 1212 alloys differed from that of conventional Al alloys in exhibiting a peak in the stress-strain curves during torsional deformation as a result of factors such as deformation heating and localized dynamic recrystallization.
- The hot ductility rose with rising temperature to a maximum at 400-500°C for 8009 and, although lower, continuously up to 600°C for FVS 1212; generally much lower ductility values than those for conventional alloys would require special caution in choosing conditions to prevent cracking during shaping. At 600°C, the exceptional ductility is combined with a low constant flow stress and a high strain rate sensitivity indicative of fine grain superplasticity.
- The activation energy for deformation was much higher than those of traditional and other RSP Al alloys, probably due to effective dislocation pinning by the high volume fraction of silicides.
- The stress multiplier (α) has a linear correlation with the slopes in the Arrhenius plots and an inverse correlation with the stress exponent n which results in Q values fairly independent of α.

REFERENCES

1. P.S. Gilman, D.J. Skinner, M.S. Zedalis and P. Gilman, *Mat. Sci. Eng.* A119, 81-86 (1989).
2. D.J. Skinner, R.L. Bye, D. Raybould and A.M. Brown, *Scripta Metal.*, 20, 867 (1986).
3. C.M. Adam, J.W. Simon, S. Longenbeck and R. Mehrabian, (ed.) *Proc. 3rd International Conference on Rapid Solidification Processing; Principles and Technologies*, Gaithersburg, MD, National Bureau of Standards, Washington, DC, 1982; p. 629.
4. S.K. Das and L.A. Davis, *Mat. Sci. Eng.*, 98, 1-12 (1988).
5. D. Shimansky, "Hot Working of High Temperature Rapidly Solidified Aluminum Alloys FVS 1212 and 8009 (FVS 0812)," A Thesis in Dept. Mechanical Engineering, presented for the Degreee of Master of Applied Science, Concordia university, Montreal, Canada, 1995.
6. D. Shimansky, H.J. McQueen, "Hot Working of Heat Resistant Rapidly Solidified Aluminum Alloy 8009", *Proc. ICAA5, Mat.Sci.Forum* 217-222, Grenoble, 1996; 1199-1202.
7. D. Shimansky and H.J. McQueen, "Hot Working of Heat Resistant Rapidly Solidified Aluminum Alloy (FVS1212)", in *Hot Workability of Steels and Light Alloys-Composites*, H.J. McQueen, E.V. Konopleva and N.D. Ryan (eds.), Met. Soc. CIM, Montreal, 1996; pp. 89-96.
8. R. Pickens, T.J. Langan, R.O. England, M. Liebson, *Metal Trans. A.*, 18A, 303-312 (1987).
9. C.M. Sellars and W.J. Tegart, *Intnl. Met. Rev.*, 17 1972; 1-24 (1972).
10. H.J. McQueen and K. Conrod, K., in: *Microstructural Control in Al Alloy Processing*, H. Chia and H.J.. McQueen eds, TMS-AIME, Warrendale, PA, 1986; pp 197-220.
11. M.J. Luton, *Workability Testing Techniques*, G.E. Dieter, ed., ASM, Metals Park, OH, 1984; pp. 95.
12. S. Fulop, K. Cadien, M.J. Luton and H.J. McQueen, *J. Test. Evaluation*, 5, 419-426 (1977).
13. H.J. McQueen, E. Evangelista, J. Bowles and G. Crawford, *Metal Science*, 18, 395-402 (1984).
14. K. Conrod and H.J. McQueen, in: *Aluminum Alloys, Their Physical and Mechanical Properties*, E.A. Starke Jr., and T.H.J. Sanders, eds., 1986; vol. 1, pp. 435-447.
15. A. Espedal, H. Gjestland, N. Ryan and H.J. McQueen, *Scandinavian Journal of Metals*, 18, 131-136 (1989).
16. E. Evangelista, A. Forcellesee, F. Gabrielli and P. Mengucci, in: *Hot Deformation of Aluminum*

Alloys, T.G. Langdon et al eds.,TMS-AIME, Warrendale, PA, 1991; pp. 121-139.

17. R. Orsund and E. Nes, in: *Annealing Processes - Recovery, Recrystallization and Grain Growth*, N. Hansen, D. Juul Jensen, T. Leffers and B. Ralph, eds., Rosklide, Denmark, 1986; p. 475.
18. H.J. McQueen, in: *Hot Deformation of Aluminum Alloys*, T.G. Langdon et al eds. TMS-AIME, Warrendale, PA, 1991; pp. 31-54, 105-120.
19. G. Avramovic-Cingara and H.J. McQueen, in: *Dispersion Strengthened Al Alloys*, Y. Kim & W.M. Griffith Eds., Met. Soc. AIME, Warrendale, PA, 1988; pp. 437-450.
20. H.J. McQueen, E. Evangelista and N.D. Ryan, *Recrystallization ('90) in Metals and Materials*, T.Chandra, ed., TMS-AIME, Warrendale, PA, 1990; pp. 89-100.
21. G.M. Pharr, M.S. Zedalis D.J. Skinner and P.S. Gilman, Rice University, Department of Materials Science, P.O. Box 1892, Houston, Texas, 77251, Allied Signal Inc., Metals and Ceramics Lab., P. O. Box 1021R. Morristown, NJ 07960.
22. D.L. Yaney, J.C. Gibeling and W.D. Nix, *Strength of Metals and Alloys ICSMA 7*, H.J. McQueen et al, eds. Pergamon Press, Oxford 1985; Vol. 3, pp. 887-892.
23. M.M. Myshlyaev, V.M. Fedorov, L.V. Fedorova and H.J. McQueen, *Hot Workability of Steels and Light Alloy-Composites*, H.J. McQueen at al., (eds.), Met.Soc. CIMM, Montreal 1996; pp. 77-88.
24. J. Zhou and J. Duszczyk, *J. Mat. Shaping Tech.*, 6, 241 (1989).
25. J. Zhou, J. Duszczyk, B.M. Korevaar and B.Verlinden., *J. Mat. Sci.*, 27, 4247-4260 (1992).
26. Y. C. Yoo, J. S . Jeon and J. H. Lee, in: *Strength of Materials (ICSMA 10)*, H. Oikawa et al., eds., Japan Inst. Metals, Sendais, 1994; pp. 831-834.